

A Differential Detector for an Ultra-wideband Communications System

Minnie Ho, V. Srinivasa Somayazulu, Jeffrey Foerster, Sumit Roy
Intel Labs
2111 N.E. 25th Ave.
Hillsboro, OR 97124-5961

Abstract- Systems using ultra-wideband (UWB) technology have been shown to achieve very high data rates (100 Mbps and above) for short-range, indoor applications. UWB signals exhibit a number of performance advantages in terms of multipath resolution and fading reduction. However, UWB systems can also exhibit significant implementation complexity in timing, synchronization, and signal correlation. This paper presents a differential detector that “rakes” in some of the multipath energy, while relaxing some of the stringent implementation requirements. We analyze the performance and the implementation of the differential detector, and compare it to a “RAKE” receiver with a correlator detector in the presence of AWGN and multipath.

I. INTRODUCTION

Considerable recent interest in ultra wideband (UWB) technology centers around its potential applicability for short-range, high-speed wireless communications while the FCC conducts an evaluation prior to approval for widespread deployment [1]. In general, there are many benefits to operating over a very wide bandwidth [2-3], one of which is the significant reduction of fading, since the short-impulse nature of the UWB waveform prevents a significant overlap of the signals. In addition, the ability to resolve individual multipath components at the receiver and “rake” in the energy of each can greatly boost the received signal-to-noise ratio. However, combining many paths using a RAKE receiver significantly increases the complexity of the implementation, and thus makes the quantitative performance vs. complexity trade-off studies necessary for choosing an appropriate receiver architecture. A sub-optimal receiver that avoids some of the complexities of the RAKE implementation uses a differential detector to combine multipath energy. In this paper, we refer to the differential detector as the DPSK receiver, and it is depicted in Figure 1. This paper describes the implementation and performance of the DPSK receiver and compares it with a RAKE receiver using a correlator detector.

II. DPSK RECEIVER PERFORMANCE ANALYSIS

In this section, the performance of the DPSK receiver in Fig. 1 is analyzed with an integrator or alternatively a low-pass filter (LPF) as shown. The input signal to the receiver is given by $r(t) = s_1(t) + n(t)$, where $s_1(t)$ is the received pulse waveform (which includes the effects of transmitter BPF and of any multipath channel), and $n(t)$ is AWGN. The received signal is passed through a wideband bandpass filter that has the same impulse response as the transmitter filter, denoted by $h(t)$. Hence $p_1(t) = s_1(t) * h(t) = s(t)$ and

$$n_1(t) = n(t) * h(t) = \int n(\tau)h(t-\tau)d\tau \quad (1)$$

The noise process $n_1(t)$ has the autocorrelation given by

$$R_{n_1}(\tau) = \frac{N_0}{2} \int h(u)h(u-\tau)du \quad (2)$$

The receiver BPF output is multiplied with a replica delayed by T_r seconds and the resulting product decomposed into the components $x(t) = x_p(t) + x_n(t)$. Here

$x_p(t) = s(t)s(t-T_r) = s^2(t)$, assuming that $s(t) = s(t-T_r)$ if the bit 0 is sent with differential encoding (Note: ISI is assumed to be negligible). Also

$$x_n(t) = s(t)[n_1(t) + n_1(t-T_r)] + n_1(t)n_1(t-T_r) \quad (3)$$

The output of the mixer is integrated over a time period T_L , $0 < T_L \leq T_r$, and a decision on the DPSK symbol is made every T_r sec. Thus, the output of the integrator, sampled at T_r spaced intervals, can be written as the sum of a signal

component $y_p(T_L) = \int_0^{T_L} s^2(t)dt$, and a noise

component $y_n(T_L) = \int_0^{T_L} x_n(t)dt = N_1 + N_2$, where

$$N_1 = \int_0^{T_L} s(t)[n_1(t) + n_1(t-T_r)]dt, \quad \text{and}$$

$$N_2 = \int_0^{T_L} n_1(t)n_1(t-T_r)dt. \quad y_n(T_L) \text{ is no longer Gaussian due to}$$

the result of the term N_2 . Rather than trying to derive the probability of error for the DPSK receiver, the signal-to-noise ratio (SNR) at the output of the integrator is examined as a function of the integrator length T_L . The noise term $y_n(T_L)$ has a mean given by:

$$\begin{aligned} E\{y_n(T_L)\} &= E\{N_1\} + E\{N_2\} \\ &= \int_0^{T_L} s(t)[E\{n_1(t)\} + E\{n_1(t-T_r)\}]dt \\ &\quad + R_{n_1}(T_r)T_L \end{aligned} \quad (4)$$

Clearly, the first of these terms is zero, since $n_1(t)$ is a zero mean random process. The second is also approximately zero, if the impulse response of the BPF has negligible autocorrelation at lag T_r seconds, which holds in situations where the PRF of the UWB signal is small compared with the UWB signal bandwidth. Thus, $E\{y_n(T_L)\} \approx 0$. The variance of $y_n(T_L)$ is then given by

$$E\{y_n(T_L)^2\} = E\{N_1^2\} + E\{N_2^2\} + 2E\{N_1 N_2\} \quad (5)$$

The first term on the right hand side can be written as

$$E\{N_1^2\} = \iint_{T_L} s(t_1)s(t_2) \left[2R_{n_{n_1}}(t_1-t_2) + R_{n_{n_1}}(t_1-t_2+T_r)R_{n_{n_1}}(t_1-t_2-T_r) \right] dt_1 dt_2 \quad (6)$$

$$\approx 2 \iint_{T_L} s(t_1)s(t_2)R_{n_{n_1}}(t_1-t_2) dt_1 dt_2$$

based on the previous discussion about $R_{n_{n_1}}(\tau)$. Next,

$$E\{N_2^2\} = \iint_{T_L} E\{n_1(t_1)n_1(t_1-T_r)n_1(t_2)n_1(t_2-T_r)\} dt_1 dt_2$$

$$= \iint_{T_L} \left[R_{n_{n_1}}^2(T_r) + R_{n_{n_1}}^2(t_1-t_2) + R_{n_{n_1}}(t_1-t_2+T_r)R_{n_{n_1}}(t_1-t_2-T_r) \right] dt_1 dt_2 \quad (7)$$

$$\approx \iint_{T_L} R_{n_{n_1}}^2(t_1-t_2) dt_1 dt_2$$

where the well-known result for the fourth moment of jointly Gaussian variables has been used [4], and previous arguments about $R_{n_{n_1}}(\tau)$ have also been employed in the approximation.

The final expression below in (8), along with (6) and (7), allows numerical computation of the output SNR for a given receiver BPF impulse response.

$$SNR_{out} = \frac{y_p^2(T_L)}{\text{Var}\{y_n^2(T_L)\}} = \frac{\left[\int_0^{T_L} s^2(t) dt \right]^2}{E\{N_1^2\} + E\{N_2^2\}} \quad (8)$$

From (8), we see that as the integration time is increased from zero, more signal energy is gathered, and the SNR_{out} increases initially. However, when the integration time extends past the pulse duration for an AWGN channel, no significant additional signal energy is gathered, while the noise terms, especially N_2 , continue to accumulate, causing the SNR_{out} to decrease.

For a multipath channel, where the UWB pulse energy will be distributed over the pulse repetition period (PRP), this argument still holds true, and it is observed that there is an optimum integration time which results in the maximum SNR_{out} at the DPSK receiver output. In Table 1 and Table 2 the behavior of SNR_{out} vs. integration time for some values of input E_b/N_0 is shown for a UWB signal in AWGN and in a multipath channel, respectively. These results are based upon the transmission of an impulse through a third-order Chebychev transmit and receiver bandpass filter with a passband of 3 to 6 GHz. The multipath channel used in generating Table 2 is a typical non-line-of-sight (NLOS) channel impulse response extracted from the measurement data in [5].

Table 1. SNR_{out} (dB) vs. integration time T_L for DPSK receiver in AWGN

E_b/N_0 (dB)	$T_L=0.25\text{ns}$	$T_L=0.5\text{ns}$	$T_L=1\text{ns}$	$T_L=2\text{ns}$	$T_L=5\text{ns}$
7	0.833	5.4019	5.3453	4.5924	2.6561
12	6.6317	10.8206	11.0506	10.8175	9.9087

Table 2. SNR_{out} (dB) vs. integration time T_L for DPSK receiver in multipath channel

E_b/N_0 (dB)	$T_L=5\text{ns}$	$T_L=10\text{ns}$	$T_L=20\text{ns}$	$T_L=25\text{ns}$	$T_L=35\text{ns}$
7	-54.8335	-5.8242	-4.4092	-4.8082	-5.234
12	-45.0191	3.1059	4.6711	4.3897	4.1032

These results predict an optimal integrator length of around 1ns for the AWGN case (corresponding to roughly the time duration of the filtered pulse), and around 20ns for the case of the multipath channel considered.

III. RAKE RECEIVER PERFORMANCE

In this paper, we compare the DPSK receiver with a "baseline" RAKE receiver (depicted in Figure 1) using a correlator detector without direct-sequence spreading. The performance of a RAKE receiver with bi-polar modulation closely follows the analysis presented in [6] for a direct-sequence spread UWB system with multipath, narrowband interference (NBI), and multiple access interference using a RAKE matched-filter receiver. Therefore, the results of [6] can be simplified, and are presented here for completeness. The final conditional probability of error, conditioned on the channel impulse response, intersymbol interference (ISI), and NBI symbols, is given by the following:

$$P_b(e/\mathbf{a}) = \frac{1}{2^2 2^{W+1}} \sum_{j=1}^{2^2 2^{W+1}} P_s(e/\mathbf{a}, \mathbf{b}_j, \mathbf{g}_j) \quad (9)$$

where

$$P_s(e/\mathbf{a}, \mathbf{b}_j, \mathbf{g}_j) = \frac{1}{2} \text{erfc}(\gamma_j) \quad (10)$$

$$\gamma_j = \frac{\sqrt{\gamma_{ave}}}{\sqrt{\mathbf{c}^T \mathbf{c}}} \mathbf{c}^T \mathbf{A}_j \mathbf{a} + \frac{1}{\sqrt{N_s L_I}} \mathbf{c}^T \mathbf{y}_j^I \quad (11)$$

$\gamma_{ave} = E_b/\eta_0$, \mathbf{c} is an L_p length column vector containing the RAKE tap coefficients, \mathbf{a} is an L length column vector of channel tap weights with spacing T_m which represents the minimum path resolution time, $N_s = B_s/B_r$ is the ratio of the equivalent UWB RF bandwidth to the pulse repetition frequency which can be considered the pulse processing gain, and $L_I = P_{ave}/P_I$ represents the signal-to-interference ratio (SIR). In the above

expression, $\mathbf{A}_j = \sum_{i=0}^Q b_{-i}^j \mathbf{E}_i$, and \mathbf{E}_i is an $L_p \times L$ matrix. Each

row, m , where $m=0, \dots, L_p-1$, of this matrix consists of a zero in all places except for a one in position $(N_r, i + p_m)$ where $N_r = T_r/T_m$, T_r is the pulse repetition period, and p_m is the path delay for the m^{th} RAKE arm. If $|N_r, i + p_m| > L$, then the row is an all zero vector.

Also, $\mathbf{y}_j^I = [y_{p_0,j}^I, y_{p_1,j}^I, \dots, y_{p_{L_p-1},j}^I]^T$ and

$$y_{p_m,j}^I = \cos(\omega_0 p_m T_m + \theta) \sum_{k=-W/2}^{W/2} g_k^j v(p_m T_m - k T_I - \tau_j)$$

represents the narrowband interference, with a carrier frequency ω_0 , symbol time T_I , random phase θ , RAKE path delays

$\{p_m T_m\}$, random delay τ_j , and "narrowband" symbol shape $v(t)$. This summation is truncated to $W=6$, which is sufficient to include the interference from adjacent "narrowband" symbols when the "narrowband" symbol time is greater than the pulse repetition period, which is the case here. Finally $g_j^I \in \pm 1$,

$b_0^j = 1$, $b_i^j \in \pm 1$, and j spans all the possible combinations of the "narrowband" interfering symbols and the ISI. The final average probability of error is then obtained by averaging over several realizations of the channel, ISI symbols, and NBI symbols.

IV. RESULTS

To perform quantitative comparisons of different receiver architectures in the same channel environment, we used estimates of the channel impulse response derived from wide-band measurements taken in a single townhouse as representative of the indoor home environment. For a more thorough description of our channel characterization, we refer to [5], but we describe some of the most relevant details as follows. After compensating for waveform distortions caused by the RF Tx/Rx filters, amplifiers, and the antennas, network analyzer data taken in the 2-8 GHz frequency band was zero-padded from 0-2 GHz, the complex conjugate of the positive frequency data was mirrored to the negative frequencies, and an inverse fast Fourier transform (IFFT) was applied to the data to yield an estimate of the real impulse response with sample spacing of 1/16 nsec (corresponding to a 16 GHz sample rate). Simulation results used this impulse response directly in Matlab[™] and Simulink[™]¹, while the analytical results required a "binning" of the data to match the discrete multipath model with a spacing of $1/B_s$, where B_s is the occupied bandwidth of the UWB impulse (3 GHz in this case). Finally, the RAKE arms for each channel were determined by stepping the correlator delay in steps of 33 psec, and choosing the maximum correlator outputs (without noise) that are separated by at least the minimum path spacing of $1/B_s$.

Figure 2 compares analysis and simulation results of the RAKE receiver for different numbers of RAKE arms, assuming maximal-ratio combining, averaged over 50 non-line-of-sight

(NLOS) channels derived from the measurements. Note that the simulations using the impulse response estimate take into account inter-pulse interference due to very closely spaced multipath and any signal distortions caused by material reflections, which are not accounted for in the analysis. These effects are more apparent in the 6- and 12-arm RAKE receiver results by noticing the difference between the simulation and analytical results. In this figure, the mean RMS delay spread of the channels is 15.4 nsec, and a PRF of 100 MHz was assumed so that the effects of ISI are also present. The measurements of the multipath in the condominium setting tended to have a smaller RMS delay spread (10-20 nsec) compared to reported measurements for an office environment (20-30 nsec for 5-30 meter separation distance) (see [5] and references therein). So, it is expected that more RAKE arms would be needed in an office environment to capture the majority of the energy present in the channel. However, this figure shows that there is still 2-3 dB to be gained by using a 6- or 12-arm RAKE compared to only a 3-arm RAKE in these typical indoor channels, which comes at the expense of increased receiver complexity. Note that the RAKE receiver results also assume perfect knowledge of the optimum path delays and amplitudes used for maximal-ratio combining.

Figure 3 compares the performance of both the DPSK and RAKE receivers averaged over 50 NLOS channels. The DPSK curves were generated using a LPF with a 100 MHz bandwidth. This figure shows that the DPSK receiver performance is severely degraded by inter-symbol interference (ISI) when the pulses are spaced 10 ns apart (PRF = 100 MHz). As the PRF is decreased to 50 MHz, the performance improves dramatically, and is close to the performance at a 5MHz PRF, suggesting that ISI is negligible when pulses are spaced more than 20ns apart for this channel. The DPSK receiver is more sensitive to ISI than the RAKE receiver, since prior symbols are mixed with the current symbol yielding an "ISI-cross-ISI" term at the output of the mixer. At a PRF of 50 MHz, the DPSK curve crosses that of the single-arm RAKE receiver at an SNR of 12 dB. For a multipath channel, there is a fundamental trade-off between receiver "noise enhancement" and multipath energy capture to consider when selecting the LPF bandwidth. For a low SNR, the "noise enhancement" is dominated by N_2 , which suggests a wider LPF would be better. However, for a high SNR, the noise is dominated by N_1 , and the multipath energy capture effect begins to dominate and allows the DPSK performance to by-pass that of the single-arm RAKE.

The DPSK receiver is more susceptible to narrow-band interference due to the "interference-cross-interference" term at the output of the mixer shows a performance degradation in the presence of an interferer when compared with the use of a RAKE receiver. However, both have the inherent processing gain of a UWB receiver, where a decrease in PRF (lower throughput) can be traded for robustness against interference. We refer to [7] for a more detailed analysis comparing the two receivers in the presence of interference. It is expected that the inherent capability of UWB to reject interference will need to be complemented with techniques such as RF notch filters or baseband signal processing techniques to maintain robustness in the presence of co-channel interference.

V. IMPLEMENTATION CONSIDERATIONS

¹ Matlab and Simulink are registered trademarks of MathWorks, Inc.

One of the challenges of a UWB system implementation is to provide very stable reference clocks for the transmitter and receiver pulse repetition frequency (PRF) generators. For example, Figure 4 shows the SNR loss of a 3 GHz wide UWB signal as a function of timing offset. The figure for the correlator receiver suggests that an overall timing offset of 25 psec, which could result from imperfect timing from the combination of jitter on the transmit and receive PRF generators, will reduce the received SNR by 1 dB. The DPSK receiver is much less sensitive to jitter on the receiver PRF clock, but still requires the pulse repetition period (PRP) at the transmitter and the fixed delay block at the receiver to be within 25 psec to prevent the 1 dB loss in SNR. It should also be noted that the delay block in the DPSK receiver is not trivial when trying to minimize amplitude and group delay distortion, especially as the delay increases.

Another challenge for the correlator/RAKE receiver is to generate an impulse that closely matches the received impulse at the input to the receiver. This means that any distortion that is caused by the transmit and receiver filters, amplifiers, or antennas, and frequency or group delay distortion caused by the channel, must be taken into account for optimal performance. Since the DPSK receiver is correlating with a delayed replica of itself (although noisy), the distortions will automatically be accounted for as long as the changes in the channel are slow relative to the PRF, which will typically be the case.

All of the results in this paper also assume perfect acquisition and synchronization. However, accomplishing this in the presence of a strong interferer and low SNR is not a trivial task. For example, the required delay needed by the RAKE for each arm is unknown at the beginning of a communications session, it must be found using some type of search procedure. The simulation results presented in this paper found the optimum RAKE arms by stepping through the delays in intervals of 33 psec, which represents 300 unknown positions to search before communications can begin. The acquisition time could be reduced (parallel search or higher sampling rates) at the expense of increased receiver complexity and power consumption.

The DPSK receiver does not have this search requirement, since it continuously correlates the received signal with a delayed, albeit noisy, replica (though a delay accurate to within about 25psec is needed). As a result, this architecture could be used to rapidly acquire the transmitted packets without a long training sequence or search algorithm. For example, if the DPSK receiver uses a 100 MHz LPF at the output of the correlator, the output can be over-sampled by a factor of 2-4, and the transmitted information can be acquired using a digital matched-filter, for example. So, for a low data rate system in order to reduce the ISI effects, this DPSK receiver architecture could be a simple and low cost alternative to the traditional RAKE receiver. In addition, the DPSK receiver could be combined with direct sequence spreading, where the de-spreading operation helps to overcome some of the inherent interference-suppression deficiencies of the DPSK receiver.

VI. CONCLUSIONS

This paper compared the performance of a conventional correlator and RAKE receiver for detecting UWB waveforms with a differential detector based upon the DPSK receiver. The analysis and results took into account realistic multipath channel realizations based upon actual channel measurements. The RAKE

results show good performance in a multipath channel that can approach the optimal BPSK performance in AWGN to within 2-3 dB, but requires on the order of 12 arms to achieve. Clearly, this will have an impact on the complexity and cost of the receiver. The DPSK receiver has a number of implementation advantages when compared with the RAKE receiver: it does not require complex acquisition and search procedures for the RAKE fingers, it does not require a priori knowledge of the pulse (and associated RF components) to correlate, and it is less sensitive to jitter on the receiver clock (although it does require the PRP at the transmitter and the delay to be closely aligned, and the delay block is not trivial to implement). However, these implementation advantages come at a cost in performance. The RAKE receiver is not saddled with the additional noise terms and the effect of the low-bandwidth LPF that are present in the DPSK receiver. Although the DPSK receiver does collect multipath energy by mixing the signal with a delayed version of itself, this performance gain only brings it to the performance level of a single-arm RAKE at low SNR and slightly better for high SNR. In addition, the DPSK receiver is shown to be much more sensitive to the effects of inter-symbol and "narrowband" interference than a RAKE due to the cross products produced at the output of the mixer, although additional equalization and other signal processing algorithms could be used to help mitigate these effects.

REFERENCES

- [1] FCC Notice of Proposed Rule Making, "Revision of Part 15 of the Commission's Rules Regarding Ultra-wideband Transmission Systems," ET-Docket 98-153.
- [2] J. Foerster, E. Green, V.S. Somayazulu and D. Leeper, "Ultra-wide Band Technology for Short or Medium-range Wireless Communications;" Intel Tech. J., Q2, 2001 (<http://developer.intel.com/technology/itj>)
- [3] M. Z. Win and R. A. Scholtz, "On the Robustness of Ultra-Wide Bandwidth Signals in Dense Multipath Environments," IEEE Comm. Letters, Vol. 2, No. 2, Feb. 1998.
- [4] J. Proakis, Digital Communications Second Edition, McGraw Hill Book Company, New York, 1989.
- [5] L. Rusch, et. al., "Characterization of UWB Propagation from 2 to 8 GHz in a Residential Environment", submitted to JSAC Spl. issue on UWB.
- [6] J. Foerster, "The Performance of a Direct-Sequence Spread Ultra-wideband System in the Presence of Multipath, Narrowband Interference, and Multiuser Interference," submitted to IEEE Conf. Ultra Wideband Systems and Tech., May 2002.
- [7] J. Foerster, et. al., "Performance Comparisons Between a RAKE Receiver and a Differential Detector for an Ultra-wideband Communications System," submitted to JSAC Spl. issue on UWB.

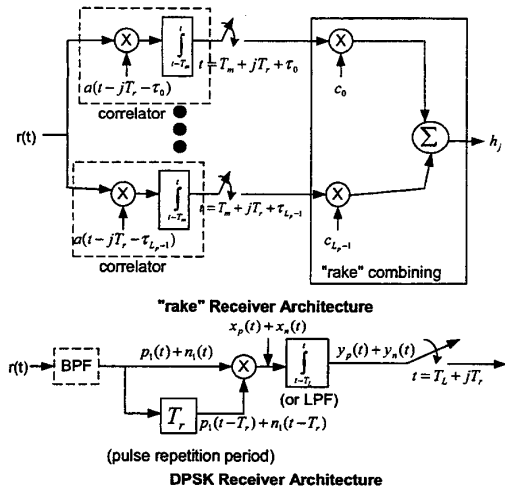


Figure 1: RAKE and DPSK Receivers for Detection of Impulsed UWB Systems

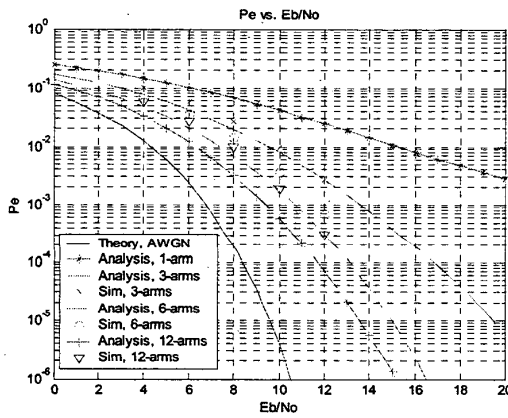


Figure 2: Comparison between analysis and simulations of a RAKE receiver averaged over 50 non-LOS channels derived from channel measurements (15.4 nsec average RMS delay spread).

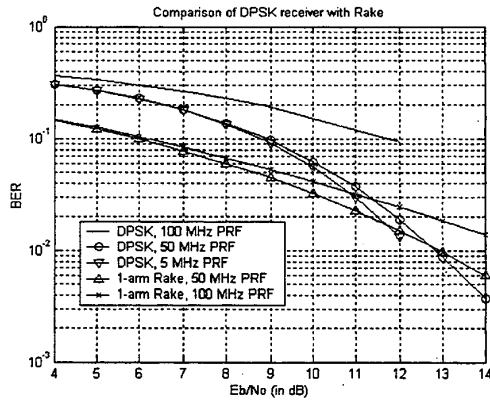


Figure 3: Simulations of a "DPSK" receiver averaged over 50 non-LOS channels derived from channel measurements (15.4 nsec average RMS delay spread)

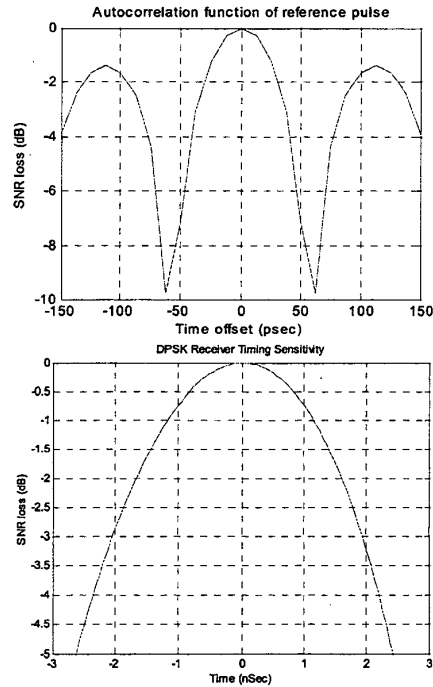


Figure 4: Sensitivity of Correlator and DPSK receivers to PRF clock time offset. Figure shows that a 1 dB loss in performance will occur with a timing error of 25 psec for the correlator receiver and about 700 psec for the DPSK receiver with a 100 MHz LPF.